Femtosecond Laser Micromachining of Fabry-Pérot Interferometers in Fused Silica for Refractive Index Sensing

João M. Maia*[a,b], Vítor A. Amorim[a,b], Duarte Viveiros[a,b], P. V. S. Marques[a,b]
[a]CAP – Centre for Applied Photonics, INESC TEC, Rua Dr. Roberto Frias, 4200-465 Porto, Portugal;
[b]Department of Physics and Astronomy, Faculty of Sciences of University of Porto, Rua do Campo Alegre, 4169-007 Porto, Portugal

ABSTRACT

A Fabry-Pérot interferometer was fabricated inside a fused silica substrate through femtosecond laser micromachining. The influence of the waveguide's writing parameters on the measured signal's quality was studied for an interferometer with a 27-μm wide cavity. Optimal signal-to-noise ratio and fringe visibility were obtained for waveguides written at 75 nJ and 50 μm/s. The same device was characterized with different refractive index liquids, and a maximum sensitivity of 1181.4±23.6 nm/RIU was obtained in the index range of 1.2962 to 1.3828 (at 1550 nm) for the spectral order $m = 46$.

Keywords: Fabry-Pérot interferometer, femtosecond laser micromachining, fringe visibility, fused silica, Mie scattering, refractive index sensing, wet etching.

1. INTRODUCTION

Femtosecond (fs) laser micromachining is a high precision fabrication technique which can be used to write three-dimensional structures that, depending on the nature of light-matter interaction, can be applied in the fields of integrated optics or microfluidics, among others[1]. In the case of fused silica, the material modification, started by a non-linear light absorption process, can result: (i) in an increase of the refractive index around the focal volume that allows the formation of optical circuits[2,3] or (ii) in an enhancement of the etch rate of the laser-affected zones relative to the bulk material, leading to an anisotropic HF (hydrofluoric acid) etching reaction that enables the fabrication of microfluidic systems[4].

Both optical circuits and microfluidic systems have already been integrated monolithically to form optofluidic devices for cell trapping or for sensing applications. By having a light beam propagating through an optical waveguide that orthogonally crosses a microfluidic channel, Bellini *et al* demonstrated trapping and stretching of red blood cells[5]. Bragheri *et al* further explored this concept and developed a cell sorter that was used to separate fluorescent from non-fluorescent particles[6]. Multiple configurations of refractive index sensors have also been shown. Maselli *et al* wrote a Bragg grating waveguide in the vicinity of a microfluidic channel[7], where light propagating through the grating evanescently interacts with the fluid inside the channel, while Crespi *et al* developed a Mach-Zehnder interferometer[8], where one of the arms of the interferometer crosses a channel. In both cases, the resonant wavelength(s) depends on the channel's refractive index. Fabry-Pérot interferometers have also been demonstrated in Foturan glass[9] where, besides being used as refractive index sensors, they can also serve as cavities in on-chip laser sources[10], thereby facilitating the development of true lab-on-a-chip devices. Given its potential, in this work, we fabricated a Fabry-Pérot interferometer and analyzed the influence of the waveguide's writing parameters on the spectrum's signal-to-noise ratio (SNR) and fringe visibility. We then characterized its response to refractive index variations of the medium inside the cavity.

2. EXPERIMENTAL PROCEDURE

2.1 Device Layout and Operation

The Fabry-Pérot interferometer is composed by an optical waveguide that is written orthogonally to a microfluidic channel, as shown in Fig. 1. Since the reflectivity at the silica-cavity interface is small, due to the low Fresnel reflection/transmission coefficients, the device can be modelled as a two-wave interferometer. The interferometer can be analyzed by measuring either the reflected or transmitted intensity ($I_{r,t}$) which is given by:

*joao.m.maia@inesctec.pt

$$I_{r,t} = I_1 + I_2 + 2\sqrt{I_1 I_2}\cos(\frac{2\pi}{\lambda}\cdot \Delta L \cdot n) \quad (1)$$

where I_1 and I_2 are the intensities of the light beams that travel though paths 1 and 2 (Fig. 1), respectively, λ is the light wavelength, ΔL is the path difference between both beams, and n is the cavity's refractive index. The reflected/transmitted intensity is maximum when the condition for constructive interference is obeyed, which occurs when the light wavelength matches the following equation:

$$\lambda_m = \frac{n\cdot(\Delta L)}{m} \quad (2)$$

where m is an integer. The sensitivity to variations in the refractive index of the cavity arises from the ensuing change of the optical path difference between both beams, which induces a shift in the resonant wavelength (λ_m), as can be inferred from equation (2).

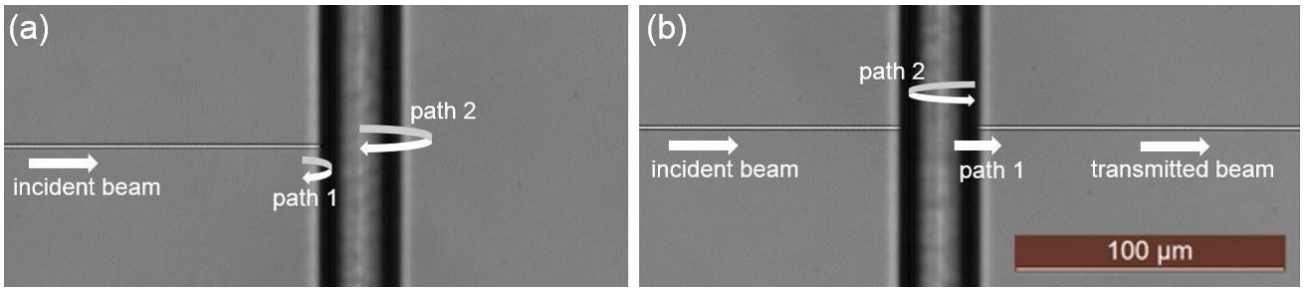

Figure 1. Low-finesse Fabry-Pérot interferometer with a fs-laser written optical waveguide fabricated orthogonal to the microfluidic channel. Paths 1 and 2 correspond to the optical paths travelled by the two interfering light beams. Figure (a) shows the configuration used to measure the reflected spectrum, while figure (b) displays the arrangement for measurement of the transmitted intensity.

2.2 Fabrication

A fiber amplified fs-laser system (Amplitude Systèmes HP) emitting a second harmonic beam at 515 nm with an approximate pulse duration of 250 fs at 500 kHz, was used to fabricate the interferometer. The linearly polarized beam was focused inside a fused silica substrate (Suprasil 1) with a 0.55 numerical aperture aspherical lens (New-Focus 5722-A-H) emplaced in a vertical piezostage (PI P-725.4CD PIFOC). The substrate was mounted on X-Y air-bearing linear stages (Aerotech ABL10100-LN) and translated in relation to the beam focus. The optical waveguide and the microfluidic channel were written sequentially to guarantee perfect alignment between both.

The optical waveguides were written 55 µm below the silica surface, with the polarization of the laser beam set parallel to the writing direction. For measuring the transmitted spectrum (Fig. 1b), waveguides crossing the 2.5-cm long substrate were written at a pulse energy of 250 nJ and scanning speed of 400 µm/s; while, to measure the reflected spectrum, 1.3-cm long waveguides placed on one side of the channel were written with energies and speeds between 50 and 200 nJ and 50 and 400 µm/s, respectively (Fig. 1a). All waveguides were written on the same direction to avoid the Quill effect.

The microfluidic channel was written from the bottom to the top by stacking multiple adjacent laser tracks, all written in the same direction, with 2 and 3 µm spacing (horizontal and vertical, respectively), at a scanning speed of 500 µm/s, pulse energy of 80 nJ and with the beam's polarization orthogonal to the scanning direction. At these conditions, the channel sidewall has low surface roughness, which leads to specular reflection of light in the channel's wall.

Wet etching was done afterwards in an ultrasonic cleaner (Branson 2510) by immersing the substrate in a 10% HF solution for 105 minutes. Due to the finite HF etching selectivity, the resulting channel width is larger at the top than at its bottom, with a deviation from the vertical of around 5°. The channel has a final width and depth of 27 and 90 µm, respectively, with the waveguides terminating around 10 µm from the channel. The substrate's edge facets were polished after etching in order to eliminate the waveguide's input section etched by the HF acid and to improve light coupling.

The Fabry-Pérot interferometer was characterized from 1490 to 1610 nm, by injecting light from a broadband source (EXFO Optical System IQ-203 with an integrated ASE source module IQ-2300) through an optical circulator and into a single-mode fiber (SMF-28 with APC termination to avoid back-reflections) that is butt-coupled to the waveguide. The reflected light is guided back into the circulator, while the transmitted light (whenever that is the case) is coupled forward into another waveguide that is also butt-coupled to a second fiber at the output facet. Both signals are detected

by an optical spectrum analyzer (Yokogawa AQ3670D), with a resolution of 1 nm. The substrate was mounted on a 5-axis stage (Elliot Martock MDE881 stage with piezocontrols Dali E-2100) for precise alignment of the optical fibers with the waveguide. Index matching (Cargille Series AA $n_D^{25^\circ C} = 1.4580 \pm 0.0002$) was used to minimize Fresnel reflections at both input/output facets.

To characterize the Fabry-Pérot's response to refractive index, the reflected/transmitted spectrum was measured for an empty channel ($n = 1.0003$ at 1550 nm) and after filling the channel with different Cargille series AAA solutions with indexes $n = 1.2962$, $n = 1.3058$, $n = 1.3154$, $n = 1.3538$, $n = 1.3731$, and $n = 1.3826 \pm 0.0002$ at 1550 nm. These liquids show negligible absorption and dispersion throughout the wavelength range tested. They were drawn into the channel by capillary forces and, after microscope observation, we confirmed no air-bubbles had been formed inside the cavity. In between measurements, the substrate was cleaned with ethanol and deionized water in an ultrasonic bath.

3. EXPERIMENTAL RESULTS AND DISCUSSION

Figure 2 shows three examples of the influence the waveguide's writing parameters and the measurement configuration, if of the reflected or transmitted intensity, have on the quality of the measured signal. In Fig. 2a, we see that, when measuring the transmitted intensity, the fringe visibility is lower than 1 dB even when the channel is empty, i.e. when the index contrast between the fused silica substrate and the cavity is maximum. This small visibility is explained by the difference between the intensities of the interfering beams: while the beam (of path 1 in Fig. 1b) is transmitted through the cavity and coupled into the forward waveguide, the beam (of path 2 in Fig. 1b) is twice reflected in the cavity before coupling to the waveguide. Given that the reflectivity at both interfaces is small, due to the low Fresnel reflection coefficients, the intensity of the former beam is much higher than the intensity of the latter and, consequently, the visibility is minimum. When the cavity's refractive index was increased by filling it with higher refractive index fluids, the visibility decreased further, due to the reduced Fresnel reflection coefficient, to the point that no modulation was observed in the transmitted spectrum. This does not occur when measuring the reflected intensity, where the visibility, for the case of an empty channel, is around 15 dB, as can be seen from Figs. 2b and 2c. In this case, both beams are only reflected once at the silica-cavity interface, and, in turn, their intensity is roughly similar, leading to a higher visibility. Note that this is only valid when the medium inside the cavity has negligible absorption, which is the case in this work.

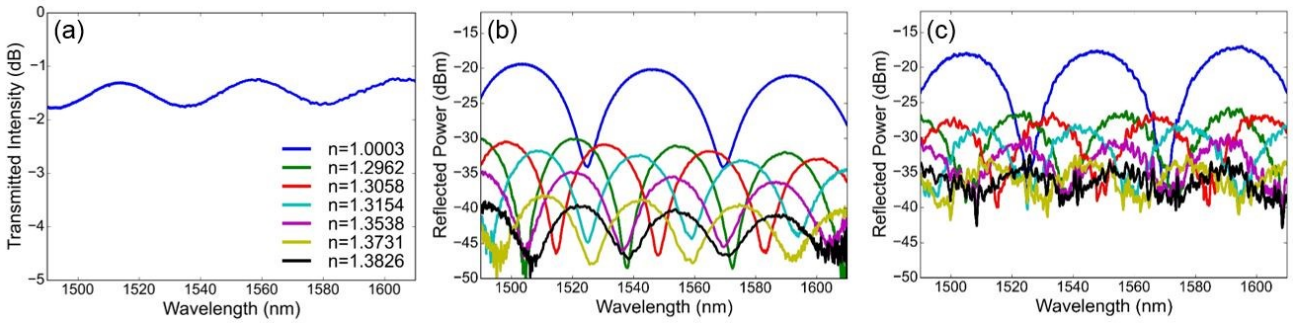

Figure 2. (a) Transmission spectrum of an empty channel. The transmitted intensity was normalized relative to the insertion losses of a similar 2.5-cm long straight waveguide. Reflected spectra, for several refractive index liquids, of a Fabry-Pérot interferometer with a waveguide written at (b) 75 nJ and 50 µm/s and (c) 200 nJ and 400 µm/s.

Comparing Figs. 2b and 2c, we also see that the waveguide's writing parameters impact the signal's quality; for instance, the spectra in Fig. 2c shows more fluctuations than the spectra displayed in Fig. 2b. Taking the Fourier transform of each spectrum, we did not observe the existence of another cavity that could be responsible for an optical beat, and concluded that these fluctuations are random. To understand their origin and relation to the waveguide's writing parameters (pulse energy and scanning speed), we then calculated the SNR of each spectrum. This was done by determining the ratio between the signal and noise root-mean squares, where the latter was determined by first smoothing the measured signal with a Savitsky-Golay filter, and then subtracting the smoothed signal from the measured one. The results are summarized in Fig. 3, where we observe that the SNR decreases when the pulse energy increases (Fig. 3a), while it is almost independent of the scanning speed (Fig. 3b). In a previous paper[11], we showed that the waveguide's propagation losses were affected by Rayleigh and Mie scattering, whose coefficients can be tuned during waveguide writing. Rayleigh scattering was shown to be negligible in the wavelength range tested in this work, while the Mie scattering coefficient increased with pulse energy and was almost independent of the scanning speed, which is similar to the

behavior observed here. We believe that in waveguides with higher Mie scattering coefficient, more inhomogeneities are formed within the waveguide, during its fabrication, that lead to random reflections and, in consequence, cause the random power fluctuations exhibited in Fig. 2c. If the writing parameters are optimized as to diminish Mie scattering, higher SNRs are obtained and the reflected spectrum is much cleaner, as depicted in Fig. 2b. Fig. 3 also shows that the SNR decreases as the cavity's refractive index approaches the fused silica's index, which is due to the lower Fresnel reflection coefficient that leads to a decrease in the signal's intensity and, therefore, of the SNR.

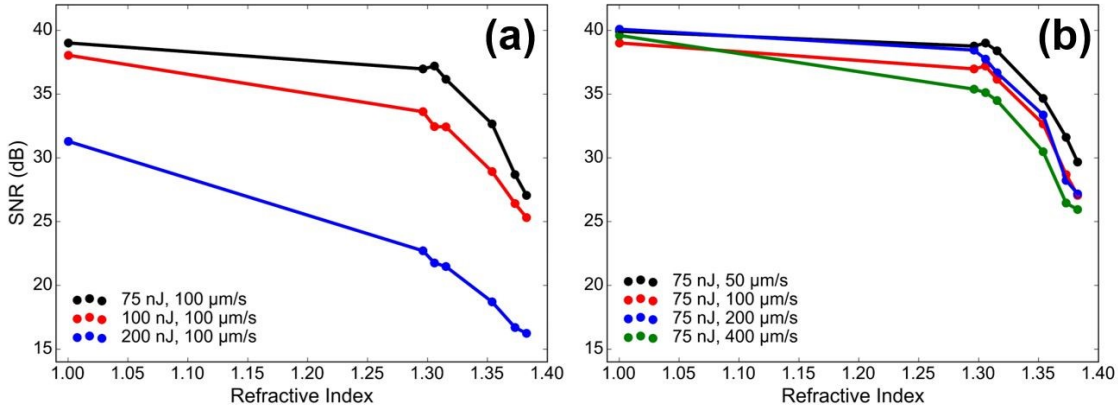

Figure 3. Signal-to-noise ratio, as a function of the cavity's refractive index for waveguides written at (a) different pulse energies and (b) different scanning speeds.

For sensing applications, higher visibilities are also desirable as it enables an easier distinction between the resonant peaks and, in turn, a measurement with better resolution. As can be seen from Fig. 4, this parameter is also dependent on the waveguide's writing conditions, increasing proportionally to the pulse energy and inversely with the scanning speed. The fringe visibility is determined by the relation between the intensity of the interfering beams, being maximum if both intensities are similar, as discussed previously. Going back to Fig. 1a, we can see that the light beam (of path 2) travels through the cavity, diverging in the process and enlarging, while the beam (of path 1) is reflected right away in the first interface and coupled back to the waveguide with minimum divergence. When coupling back into the waveguide, the amount of light that is coupled depends on the waveguide's acceptance angle. Given that both beams have different radiuses, their intensity will only be similar if the acceptance angle is high enough. The latter parameter is related to the index modification induced by the fs-laser: higher index modifications lead to a higher numerical aperture and, consequently, acceptance angle. Previously[11], we showed that writing at higher pulse energies or at lower scanning speeds results in a higher index modification, similar to what we observe in Fig. 4. Therefore, we suspect that the lower visibilities observed at lower pulse energies and at higher scanning speeds are a direct consequence of the waveguide's low numerical aperture. Nonetheless, further studies are necessary to understand how the channel's shape and the waveguide-to-channel sidewall distance also affect the visibility.

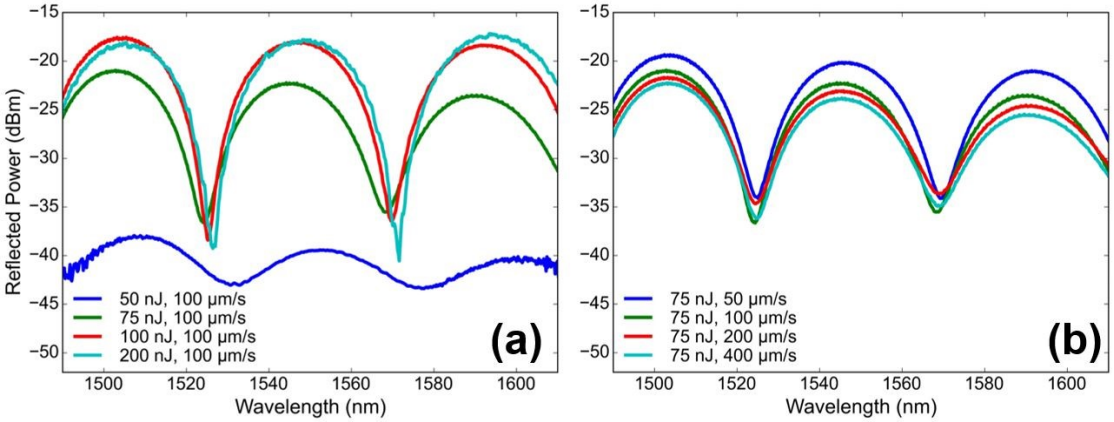

Figure 4. Reflected spectra of a Fabry-Pérot interferometer for waveguides written at (a) different scanning speeds and (b) different pulse energies. In all measurements, the cavity is empty corresponding to an index $n = 1.0003$.

All things considered, the SNR and fringe visibility were found optimal when the optical waveguide is written with a pulse energy of 75 nJ at a scanning speed of 50 µm/s. Therefore, we used a waveguide written under these conditions to characterize the response of a Fabry-Pérot interferometer, with a 27-µm wide cavity, to refractive index variations inside the channel. Figure 5 shows that this response is linear, with a maximum sensitivity of 1181.4±23.6 nm/RIU (refractive index unit) having been obtained in the index range of 1.2962 to 1.3828 (both at 1550 nm) for the order m equal to 46. We also observe a decrease of the sensitivity $(d\lambda/dn)$ with the spectral order m, which is expected from equation (2).

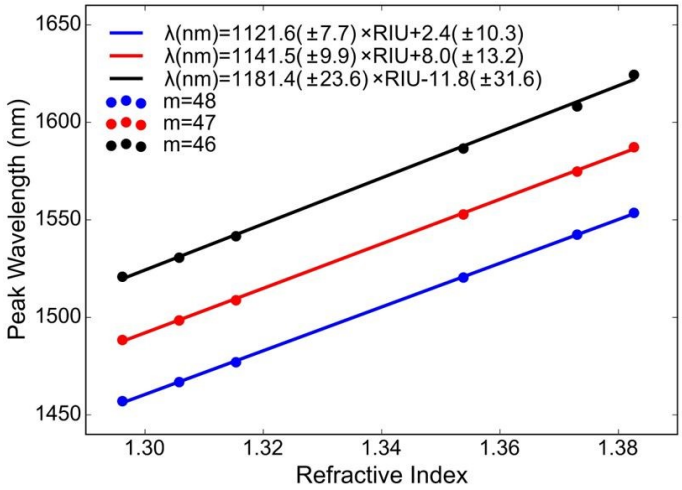

Figure 5. Peak wavelength as a function of the refractive index, for three different spectral orders m.

4. CONCLUSION

In this work, we fabricated a Fabry-Pérot interferometer in a fused silica substrate and analyzed the influence of the pulse energy and scanning speed, used to write the optical waveguide, on the measured signal's quality. The signal-to-noise ratio was found to decrease with the increase in pulse energy. This behavior is due to the increase in the Mie scattering coefficient, which manifests as inhomogeneities within the waveguide that introduce random reflections throughout it, leading to power fluctuations in the reflected signal. The visibility was also found to be lower when writing at higher scanning speeds or at lower pulse energies, which we believe to be a consequence of the waveguide's lower acceptance angle which, in turn, leads to a smaller percentage of light being recoupled back into it. For a 27-µm wide cavity, the signal-to-noise ratio and fringe visibility were found optimal when the optical waveguide was written at 75 nJ and 50 µm/s, and with the fs-laser beam polarization set parallel to the scanning direction. The same device was characterized with different refractive index liquids, and a maximum linear sensitivity of 1181.4±23.6 nm/RIU was determined in the 1.2962 to 1.3824 index range (at 1550 nm) for the spectral order $m = 46$, corresponding to a minimum resolvable refractive index variation of approximately 8.5×10^{-4}.

ACKNOWLEDGMENTS

This work was supported by Fundação para a Ciência e Tecnologia through grant no. SFRH/BD/133095/2017 and by project "NanoSTIMA: Macro-to-Nano Human Sensing: Towards Integrated Multimodal Health Monitoring and Analytics/NORTE-01-0145-FEDER-000016", financed by the North Portugal Regional Operational Programme (NORTE 2020), under the PORTUGAL 2020 Partnership Agreement, and through the European Regional Development Fund (ERDF).

REFERENCES

[1] Tan, D., Sharafudeen, K. N., Yue, Y. and Qiu, J., "Femtosecond laser induced phenomena in transparent solid materials: Fundamental and applications," Progress in Materials Science 76(1), 154-228 (2016).

[2] Choudhury, D., Macdonald, J. R. and Kar, A. K., "Ultrafast laser inscription: Perspectives on future integrated applications," Laser and Photonics Reviews 8(6), 827-846 (2014).
[3] Ams, M., Dekker, P., Gross, S. and Withford, M. J., "Fabricating waveguide Bragg gratings (WBGs) in bulk materials using ultrashort laser pulses," Nanophotonics 6(5), 743-763 (2017).
[4] Hnatovsky, C., Taylor, R. S., Simova, E., Rajeev, P. P., Rayner, D. M., Bhardwaj, V. R. and Corkum, P. B., "Fabrication of microchannels in glass using focused femtosecond laser radiation and selective chemical etching," Applied Physics A: Materials Science and Processing 84(1-2), 47-61 (2006).
[5] Bellini, N., Vishnubhatla, K. C., Bragheri, F., Ferrara, L., Minzioni, P., Ramponi, R., Cristiani, I. and Osellame, R., "Femtosecond laser fabricated monolithic chip for optical trapping and stretching of single cells," Optics Express 18(5), 4679-4688 (2010).
[6] Bragheri, F., Minzioni, P., Martinez Vazquez, R., Bellini, N., Paiè, P., Mondello, C., Ramponi, R., Cristiani, I. and Osellame, R., "Optofluidic integrated cell sorter fabricated by femtosecond lasers," Lab on a Chip 12(19), 3779-3784 (2012).
[7] Maselli, V., Grenier, J. R., Ho, S. and Herman, P. R., "Femtosecond laser written optofluidic sensor: Bragg Grating Waveguide Evanescent probing of Microfluidic channel," Optics Express 17(14), 11719-11729 (2009).
[8] Crespi, A., Gu, Y., Ngamsom, B., Hoekstra, H. J. W. M., Dongre, C., Pollnau, M., Ramponi, R., Van Den Vlekkert, H. H., Watts, P., Cerullo, G. and Osellame, R, "Three-dimensional Mach-Zehnder interferometer in a microfluidic chip for spatially-resolved label-free detection," Lab on a Chip 10(9), 1167-1173 (2010).
[9] Lin, C.-H., Jiang, L., Ziao, H., Chai, Y.-H., Chen, S.-J. and Tsai, H.-L., "Fabry-Perot interferometer embedded in a glass chip fabricated by femtosecond laser," Optics Letters 34(16), 2408-2410 (2009).
[10] Simoni, F., Bonfadini, S., Spegni, P., Lo Turco, S., Lucchetta, D. E. and Criante, L., "Low threshold Fabry-Perot optofluidic resonator fabricated by femtosecond laser micromachining," Optics Express 24(15), 17416-17423 (2016).
[11] Amorim, V. A., Maia, J. M., Viveiros, D. and Marques, P. V. S., "Loss Mechanisms of Optical Waveguides Inscribed in Fused Silica by Femtosecond Laser Direct Writing," Journal of Lightwave Technology 37(10), 2240-2245 (2019).